



## Ring formation from a drying sessile colloidal droplet

Wenbin Zhang, Tongxu Yu, Longguang Liao, and Zexian Cao

Citation: *AIP Advances* **3**, 102109 (2013); doi: 10.1063/1.4824741

View online: <http://dx.doi.org/10.1063/1.4824741>

View Table of Contents: <http://scitation.aip.org/content/aip/journal/adva/3/10?ver=pdfcov>

Published by the *AIP Publishing*

---

### Articles you may be interested in

[Dynamics of evaporative colloidal patterning](#)

*Phys. Fluids* **27**, 092105 (2015); 10.1063/1.4930283

[Precision control of drying using rhythmic dancing of sessile nanoparticle laden droplets](#)

*Appl. Phys. Lett.* **104**, 163108 (2014); 10.1063/1.4873394

[Evaporation of a sessile liquid droplet from the shear or flexural surfaces of a quartz tuning fork](#)

*J. Appl. Phys.* **114**, 074511 (2013); 10.1063/1.4818954

[Nanoparticle ring formation in evaporating micron-size droplets](#)

*Appl. Phys. Lett.* **84**, 4774 (2004); 10.1063/1.1759378

[Drying of acoustically levitated droplets of liquid–solid suspensions: Evaporation and crust formation](#)

*Phys. Fluids* **14**, 2289 (2002); 10.1063/1.1483308

---

The image shows the cover of the journal 'AIP Applied Physics Reviews'. It features a blue and orange color scheme with a molecular structure in the background. The text 'NEW Special Topic Sections' is prominently displayed in white. Below it, 'NOW ONLINE' is written in orange, followed by 'Lithium Niobate Properties and Applications: Reviews of Emerging Trends' in white. The AIP Applied Physics Reviews logo is in the bottom right corner.

## NEW Special Topic Sections

**NOW ONLINE**  
Lithium Niobate Properties and Applications:  
Reviews of Emerging Trends

**AIP** Applied Physics Reviews

## Ring formation from a drying sessile colloidal droplet

Wenbin Zhang, Tongxu Yu, Longguang Liao, and Zexian Cao<sup>a</sup>

*Institute of Physics, Chinese Academy of Sciences, 100190 Beijing, China*

(Received 1 May 2013; accepted 25 September 2013; published online 4 October 2013)

Ring formation from drying sessile colloidal droplets ( $\sim 1.0$  mm in size) containing microparticles of silicon or polystyrene was investigated with video microscopy. Results show that ring formation begins at the pinned contact line with the growth of an annular nucleus in a line by line way, which recedes inward albeit only slightly, followed by stacking of particles when the flow velocity becomes sufficiently large. The central height of the droplet decreases linearly with evaporation time, which implies that in the early stage, the number of particles arriving at contact line increases with time in a power law  $N \propto t^{3/(1+\lambda)}$ , where the parameter  $\lambda$ , according to Deegan's evaporation model, is related to the contact angle via  $\lambda = \frac{\pi-2\theta_c}{2\pi-2\theta_c}$ . Experimental values of  $\lambda$  agree well with model calculation for small contact angles, but are relatively smaller in the case of large contact angles. 'Amorphization' mechanism for the deposit at different stages of evaporation is discussed. Marangoni flow in a droplet on heated substrate introduces a desorption path for particles along the liquid surface, which can partially resolve the ring. Residual particles floating on the liquid surface may leave behind a homogeneous monolayer coating inside the dried spot. A "jump" in the droplet surface area at later stage of evaporation seems inevitably to cause a depletion zone of particles next to the ring. These results may be helpful for the development of strategies towards suppression of coffee ring effect and/or obtaining homogeneous coatings from drying colloidal suspension. © 2013 Author(s). All article content, except where otherwise noted, is licensed under a Creative Commons Attribution 3.0 Unported License. [<http://dx.doi.org/10.1063/1.4824741>]

### I. INTRODUCTION

Solid particles dispersed in an evaporating sessile droplet will migrate to the edge of the droplet and form a solid ring at the three phase contact line, leaving behind ring-like stains. This phenomenon is ubiquitous that it occurs in a robust way for a wide range of surfaces, solvents, and solutes. Deegan and co-workers explained this deposition of particles at the contact line, dubbed the coffee ring effect, with the outward flow driven by evaporation and geometrical constraint.<sup>1</sup> They showed that a ring, instead of a uniform spot, is formed because the contact line of the droplet is pinned at the substrate, and the solvent must therefore be drawn from the center to the edge to keep the contact line fixed as evaporation proceeds. This evaporation-driven flow drags the dispersed particles towards the contact line, where they deposit as the solvent dries out.

The coffee ring effect has been observed in diverse solutions with the solute ranging from large colloids,<sup>2</sup> nanoparticles<sup>3,4</sup> to polymers,<sup>5</sup> and even to individual molecules.<sup>6,7</sup> Mineral rings left on washed glassware or sweat stained clothes are convenient examples of physical systems displaying such a behavior. Understanding the formation of the ring-like patterns from a colloidal droplet is important for many applications such as printing,<sup>8-10</sup> genotyping,<sup>11</sup> and colloidal self-assembly,<sup>12,13</sup> for which the distribution of the solute during drying process has to be put under control. Recently it was even demonstrated that the pattern formed by drying of biological fluids can be used as a means of disease diagnosis.<sup>14</sup> On the other hand, the coffee ring effect is essentially a disturbing

<sup>a</sup>To whom correspondence should be addressed. E-mail: [zxcao@iphy.ac.cn](mailto:zxcao@iphy.ac.cn)



factor for various processes where it often has the need to coat a solid surface in uniform thickness. The segregation effect is there highly undesirable.

The deposition process and the resulting patterns from a drying colloidal droplet are subject to various physical and chemical constraints. For instance, the wettability and surface roughness of the substrate are important factors in determining the geometry of an evaporating drop.<sup>15–18</sup> In the presence of a temperature gradient or a surfactant concentration gradient, a convective flow arises within the drop,<sup>19,20</sup> which contributes to the emergence of very complicated, even fractal-like, deposit patterns. Moreover, stick-slip motion of the contact line results in the formation of multi-ring stains.<sup>21</sup> Many strategies have been proposed and tested for avoiding the coffee ring effect, including the addition of surfactant to modify the surface/interface energy,<sup>20,22</sup> the induction of a convective flow,<sup>19</sup> or changing the particle shape,<sup>23–25</sup> etc.

Up to now, much effort has been devoted to the observations or measurements of coffee ring effect at macroscopic level, while the microscopic and dynamic investigation over this very intriguing effect still leaves much to be done. Some details concerning the ring growth, e.g. how the particles come to the pinned contact line to initiate the ring growth, remain to be clarified and specified. In the current work, we investigate the ring formation process from sessile colloidal droplets by direct microscopic visualization with the aid of video microscopy and high-speed photography. The initial stage of the ring growth will be analyzed based on the images and the counting of arriving particles, and then compared with model calculation. Also the effect of Marangoni flow in modifying the particle distribution in the dried spots was investigated, which can provide useful clues for obtaining monolayer deposition by manipulation of the ring formation process.

## II. EXPERIMENTAL

Colloidal solutions of silica particles with a diameter of 1.0 and 5.0  $\mu\text{m}$ , and polystyrene particles with a diameter of 0.5, 1.0 and 5.0  $\mu\text{m}$  (Colloidal laboratory, China University of Petroleum), were used in this work. The solutions with a mass concentration between 0.001% and 1% were prepared by diluting the purchased solution (original mass concentration 1%) with doubly deionized water. Before each measurement the solution was ultrasonicated for 30 minutes to break the aggregates of particles. The substrates are the soda-lime glass and bulk silicon with a native oxidized surface, which had been sequentially cleaned in acetone, ethanol and deionized water. To monitor the process of the ring growth, an Olympus BX51 microscope with a set of various objective lenses (ranging from 5 $\times$  to 100 $\times$ ) was used. Solution droplets were laid on the substrate under the guidance of microscope, the volume is chosen to be about 0.5  $\mu\text{L}$ , forming a cap of which the base is approximately 1 mm in diameter. Most experiments were performed at room temperature, with a relative humidity of 25%. Moreover, a high speed camera (Giga view, SVSI) was used to monitor the side view of the droplet, which can obtain a dynamic record of the varying droplet profile during evaporation. Effect of Marangoni flow on ring formation was investigated at substrate temperatures up to 130°C.

## III. RESULTS AND DISCUSSION

With all the two kinds of particles in three distinct sizes, coffee ring effect could be observed on both bulk silicon and the soda-lime glass. It was found that the evaporation experiment could be done with the colloidal droplets of largely differing concentrations, thus solutions of various concentrations can be chosen to facilitate the observation for different research purposes. As similar behaviors can be observed in the various colloidal systems prepared for the current investigation, the discussion below is mainly exemplified by the solution of 1.0  $\mu\text{m}$  silica particles, in proper concentrations suitable for the specific observations.

Figure 1 presents the profile variation for a drying colloidal droplet on the glass substrate, which is water suspension of 1.0  $\mu\text{m}$  large silica particles with a mass concentration of 0.01%. The profiles of the drying droplet were measured successively at each 30 seconds from the side-view image, which are expected to provide some information to infer the evaporation process. The curves in Figure 1 are the measurement for the first three minutes; those data at later moments for the vanishing droplet (not shown here) are subject to large inaccuracy. We see that the contact line in the

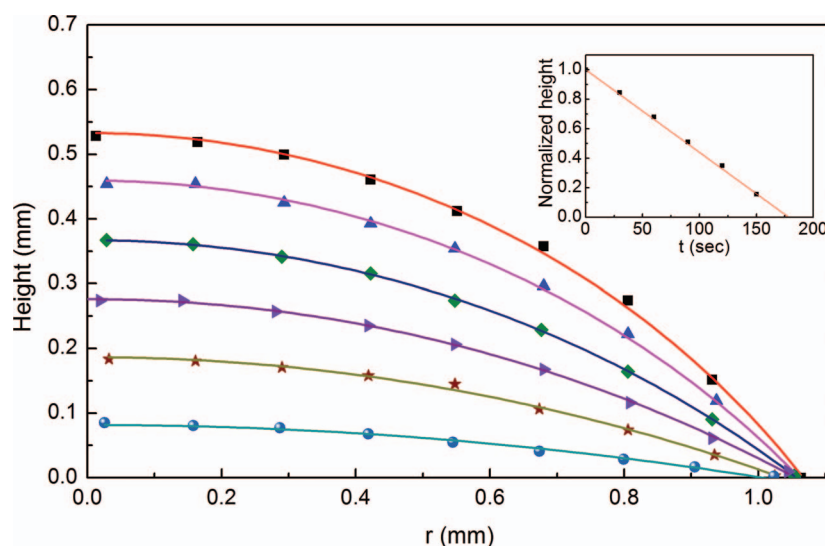


FIG. 1. Profile of an evaporating droplet on silicon at successive time moments in an interval of 30 seconds. The profiles (solid line) were constructed from the data of height of the interface vs. distance from the center read from photographs of the droplet. The droplet is water suspension of silica particles of  $1\ \mu\text{m}$  in size, with a mass concentration of 0.01 %. The initial volume is about  $0.5\ \mu\text{L}$ , and the initial contact angle is  $53.2^\circ$ . Inset shows the normalized height  $h(0,t)/h(0,0)$  which reveals excellent linearity.

first 150 s is immobile, i.e., pinned to the substrate. A slight receding of the contact line becomes noticeable at 200 s.

For a droplet drying on a solid substrate, there are two evaporation modes:<sup>26</sup> the pinning mode in which the radius of the base stays unchanged while the contact angle becomes smaller, and the depinning mode in which the base shrinks but the contact angle remains constant. The droplets here concerned remain pinned on the substrate till the end of evaporation process, leaving behind a ring-like deposition pattern. As the substrate surface is very clean, this seems arise from self-pinning,<sup>2</sup> i.e., the contact line is initially held by the surface roughness or chemical heterogeneities of the substrate. Once the contact line is pinned at the substrate, a replenish flow will move to the edge of the droplet, as evaporation proceeds, to minimize the droplet surface, and this flow conveys the particles to the contact line. The accumulation of particles as a consequence in turn strengthens the pinning of contact line.

The size of all the droplets here concerned is smaller than the capillary length of clean water, which is around 2 mm at normal temperature and pressure, so that the surface tension which tends to make droplet spherical is dominant rather than the gravity which tends to flatten the droplet. Hence, the droplet profiles can be well approximated with a spherical cap, as confirmed by data fitting in Figure 1. The central height of the evaporating colloidal droplet is found to decrease linearly with the evaporating time. Thus the lifetime of the droplet can be determined by extrapolating the fitting curve. The inset in Fig. 1 displays the time evolution of the central height of the droplet, which can be linearly fitted with the function  $h(0, t) = h(0, 0)(1 - t/t_f)$ ,  $t_f \approx 178.4$  s. This calculated lifetime of the droplet is in excellent agreement with the value of 178.6 s judged from the video record of ring formation process under microscope. This linear relationship will be later employed in obtaining the time dependence of particles joined into the ring structure.

The dried colloid droplet left behind a spot encircled by a ring comprising of deposited colloidal particles. Figure 2(a) shows the spot obtained by drying a sessile droplet on soda-lime glass slide, which primarily contains silica particles of  $1.0\ \mu\text{m}$  in size, and with a concentration of 0.1%. The base of the droplet is roughly a circle of 1.0 mm in diameter. Obviously, most of the particles accumulated along the pinned perimeter of the dried spot to form a ring. Under enlarged magnification, we can see that the ring is about  $40\ \mu\text{m}$  wide, manifesting a multilayered structure (Figs. 2(b)–2(d)). Inside the circular spot, some sporadic dark points can be viewed, which are equally the aggregates of

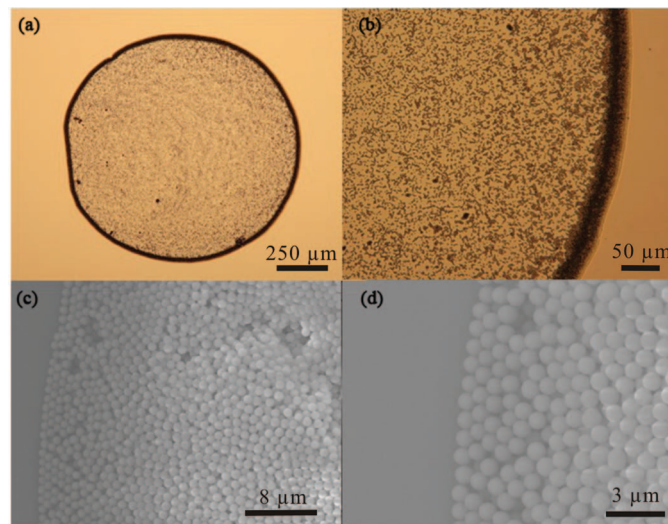


FIG. 2. Optical (a–b) and SEM (c–d) images of a ring deposition resulting from evaporation of a sessile colloidal droplet containing silica particles. (a) A ring of piled particles is visible at the three phase contact line of the droplet; (b) The enlarged image reveals that over 90% of the particles in total are deposited at the droplet's edge; (c–d) The packing of the silica particles in the ring structure. Colloidal mass concentration: 0.1 %, and initial volume is  $\sim 0.5 \mu\text{L}$ , and the initial contact angle is  $25^\circ$ .

particles as the ring at periphery. By counting the number of particles, it was estimated that only about 9.3 percent of the total particles are left inside the spot, or in other words, most of the particles in the droplet are now found in the ring structure. This can be directly viewed from the enlarged photographs which show that in contrast to the close packing of particles in the ring, the deposit inside the spot is generally monolayer thick.

The ring is the result of self-assembly of the particles, which has a ridge-like profile. In the vicinity of the contact line, the particles are close-packed and the pattern, loosely speaking, can be taken as an ordered crystal. At the same time, on the side of the ring facing the droplet center, particles form a non-compact structure with decreasing thickness. More defects and delamination are visible in this part (Fig. 2(d)). This can be viewed as an order-to-disorder transition in the ring,<sup>27</sup> which originates in the accelerated flow velocity and reduced availability of particles at the later stage of evaporation. The video for the formation process of the ring reveals that at the beginning, the silica particles gather at the edge of the droplet in a line by line way to form a 2D close-packing nucleus (Fig. 3). In this process, the shrinking droplet drives the 2D nucleus a little bit inward, so that the actual ring size is slightly smaller than the base of the original droplet. Of course, the inward motion of the annular nucleus implies a reduced particle separation, thus this inward shift can only proceed to a very limited range (Cf. Fig. 1). When the replenish flow becomes fast enough, more particles come to the edge, and stacking of particles on precedent layers follows, which destroys the monolayer growth mode. At this stage, the newcomers may appear as dimer or even small cluster, and they have less chance to find a proper position to accommodate into the deposit. Thus the structure obtained at this stage is rather amorphous. Noticeably, even the first-formed ordered deposit will later also be amorphized. When the contact angle becomes sufficiently small, the surface tension exerts directly on the particles in the edge that the deposit is displaced irregularly inward as a whole, and the ordered region in the edge is obviously distorted, see the right two panels in Fig. 3.

With the microscopic video record the number of particles arriving at the contact line as droplet evaporates can be counted, so as to infer the growth process of the ring. In order to make a precise counting, a sessile droplet of diluted solution of silica particles (particle size  $1.0 \mu\text{m}$ , mass concentration is 0.03%) was investigated on silicon substrate at room temperature, and the particle number vs. time curve is show in the inset of Figure 4. Following Deegan's evaporation model for a sessile droplet (Cf. Fig. 3 of Ref. 2) of which the shape is assumed to be a spherical



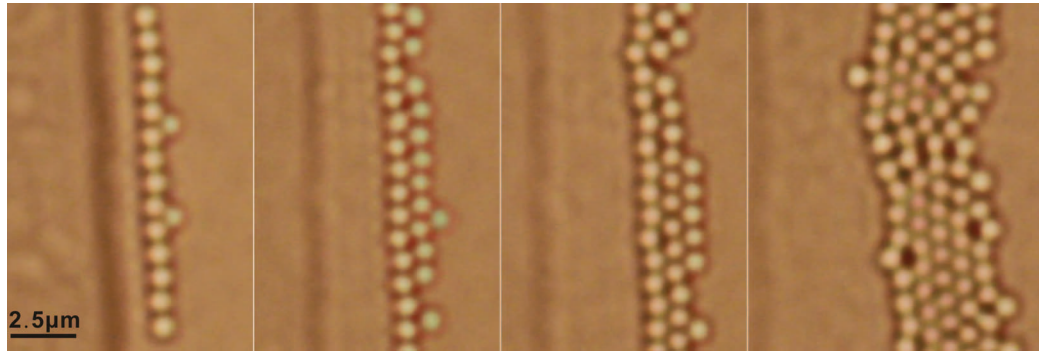


FIG. 3. Initial stage of ring formation from a drying colloidal droplet on glass substrate. The mass concentration of solution is 0.01%, and the contact angle of the droplet is  $\sim 25^\circ$ . The evaporation time (from left to right) is 20, 80, 100, and 140 s, and number of particles is 16, 29, 41, and 84, respectively.

cap,  $h(r, t) = \sqrt{[\frac{h^2(0,t)+R^2}{2h(0,t)}]^2 - r^2} - \frac{R^2-h^2(0,t)}{2h(0,t)}$ , where  $R$  is the radius of the droplet's base and  $h(0,t)$  is the height at the droplet center, the rate of change for the fluid in an infinitesimal annular element at radial distance  $r$  from the center of the droplet is equal to the net flux of liquid into the column minus the amount of mass evaporated from the surface of the element, thus it has  $\rho \frac{\partial h}{\partial t} = -\rho \frac{1}{r} \frac{\partial}{\partial r}(rhV) - J_s(r, t)\sqrt{1 + (\frac{\partial h}{\partial r})^2}$ , where  $\rho$  is the density of the liquid,  $V(r, t)$  is the velocity of the radial flow inside the fluid,  $J_s(r, t)$  denotes the rate of evaporation. Suppose that the contact angle  $\theta_c$  is small that at the edge of the droplet  $h \sim (R - r)\theta(t)$ , and there the  $\partial h/\partial t$  term also can be ignored, then by integration the velocity of the radial flow can be obtained, i.e.,  $V \propto (R - r)^{-\lambda}$ , where the parameter  $\lambda$  is determined by the contact angle via  $\lambda = \frac{\pi - 2\theta_c}{2\pi - 2\theta_c}$ .<sup>2</sup> For a particle initially located at  $r$ , the time it takes to reach the contact line is given by  $t \sim \int_r^R dr'/(R - r')^{-\lambda} \sim (R - r)^{1+\lambda}$ . By this time of  $t$ , the particles that are within the distance of  $(R - r)$  from the contact line will be incorporated into the ring, thus a power law for the number of particles coming to the edge at time  $t$  is established, i.e.,  $N \sim (R - r)^3 \sim t^{3/(1+\lambda)}$ . The data in the inset of Fig. 4 can be well fitted with this  $N$ - $t$  relationship, where  $\lambda$  is 0.14. According to this relationship, the growth rate of the ring will increase as evaporation proceeds, which agrees with the video record of the ring growth process. This certainly originates in the increasing replenish flow velocity  $V$ .

The ring growth rate is expected to depend on the contact angle of the primary sessile droplet via the parameter  $\lambda$ . For a colloidal droplet exhibiting a larger contact angle  $\theta_c$ ,  $\lambda$  is smaller, thus the exponent  $\frac{3}{1+\lambda}$  is larger, which implies a rapid growth of the ring. To verify this point, we put several droplets of the same solution on glass and silicon substrate, respectively. Following the same procedure presented above, the values of  $\lambda$  for seven droplets in total are summarized in Figure 4. For the four droplets on silicon substrate, the values of  $\lambda$  are 0.142, 0.179, 0.141, and 0.166. The corresponding  $\lambda$  value calculated from the contact angle of  $69.8^\circ$  is 0.18. As for the other three droplets on glass substrate, their values of  $\lambda$  are 0.437, 0.432, and 0.419, and the corresponding  $\lambda$  value calculated from the contact angle of  $25.3^\circ$  is 0.42. We see that the parameter  $\lambda$  in the power law for the  $N$ - $t$  relationship agrees well with that calculated from the contact angle when, as for droplets on glass, the contact angle is smaller. In the case of large contact angle, the value of  $\lambda$  calculated from the contact angle seems much larger than determined from the ring growth experiment. A large contact angle implies that there will be more particles arriving at the contact line for the same magnitude of flow velocity.

A remarkable feature of coffee ring growth presented above is that at the initial stage the ring growth proceeds in a line-by-line mode, in analogue to the layer-by-layer mode by film growth, which leaves behind a close-packed arrangement of particles at the outermost edge. The line-by-line mode is very favorable for obtaining ordered structures by colloidal growth. However, we noticed that on the particles in the outermost edge, even the contact line has trespassed them to recede inward, they are still covered by a liquid membrane. At the end of evaporation, there is no more

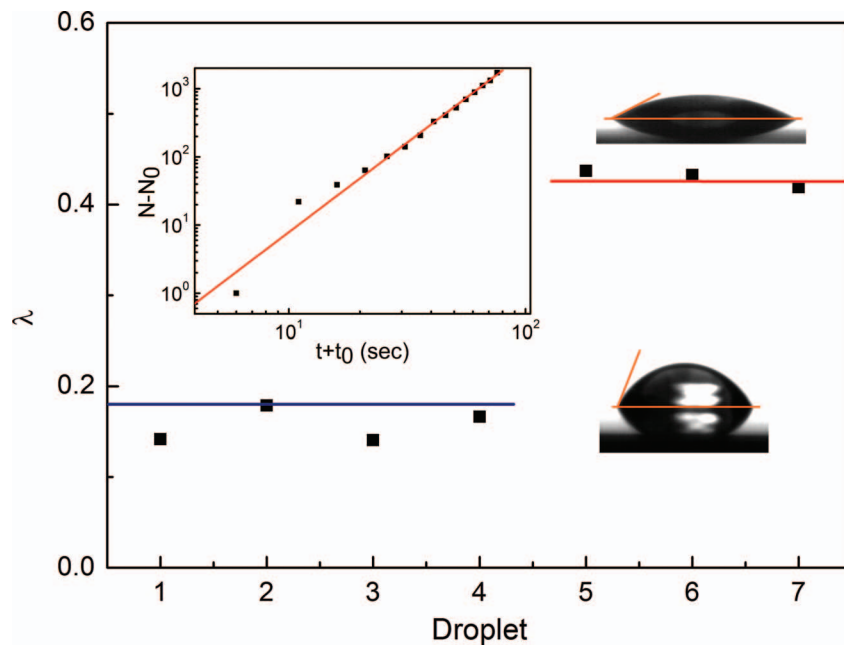


FIG. 4. Values of  $\lambda$  in the power law of  $N \propto t^{3/(1+\lambda)}$  for colloidal droplets on silicon (Nos. 1–4) and on glass (Nos. 5–7) substrates. The typical images of the droplets reveal a contact angle of  $69.8^\circ$  and  $25.3^\circ$ , respectively. Colloidal mass concentration: 0.03 %; initial volume:  $0.5 \mu\text{L}$ . The lines represent the values of  $\lambda$  calculated from the corresponding contact angle. Inset shows an exemplary  $N$ - $t$  curve in the form of log-log plot obtained on silicon, where  $\lambda$  is 0.14.

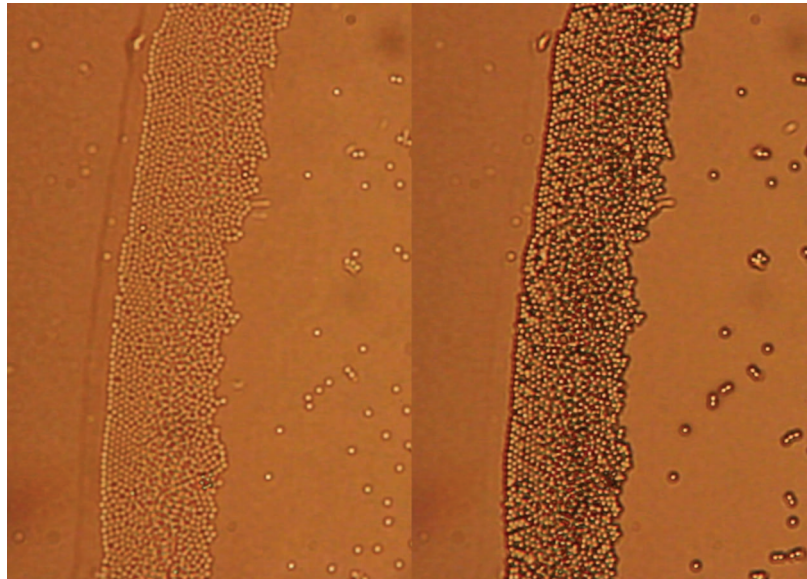


FIG. 5. Ordered particle deposition (left panel) distorted at the last moment of evaporation due to the breaking of liquid membrane over the particles. Colloidal mass concentration: 0.05%, initial volume:  $\sim 0.5 \mu\text{L}$ .

sufficient liquid to sustain this membrane that it commits sudden break-up, which generally first occurs at places among three neighboring particles. This effect is so violent that it can displace the deposited particles to a degree that the ordered structure previously obtained can be ruined (Figure 5). Countermeasure should be called in to avoid this disturbance when growing colloidal crystals via evaporation.

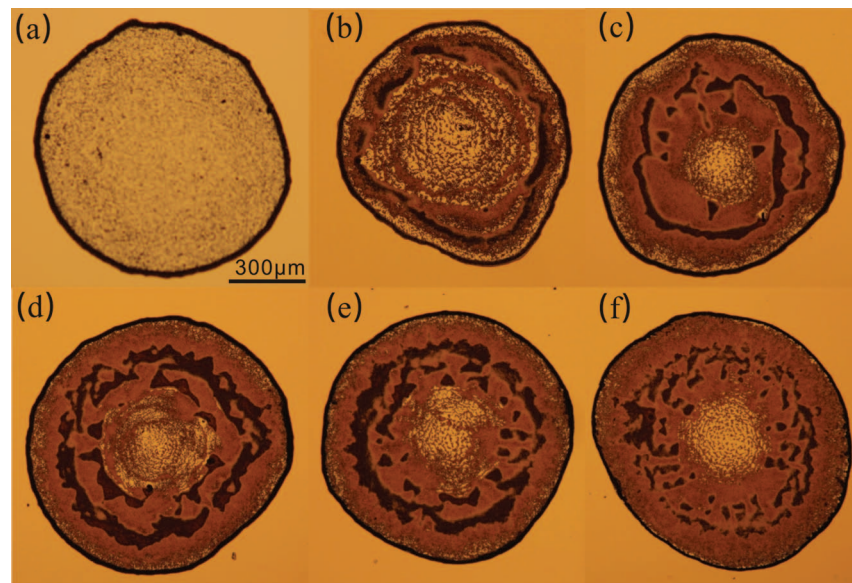


FIG. 6. Optical images of the ring deposition on glass substrates obtained at a substrate temperature of (a) 25°C, (b) 50°C, (c) 60°C, (d) 80°C, (e) 100°C and (f) 130°C. Colloidal mass concentration: 0.25%, initial volumes:  $\sim 0.5 \mu\text{L}$ .

In order to suppress the ring formation from a drying droplet, other flows in addition to that caused by evaporation have to be introduced. It is well known that Marangoni flow will be induced by the presence of a temperature gradient in the droplet, and this flow can modify the deposit pattern.<sup>19</sup> We put some colloidal droplets on a heated glass substrate to observe the drying process by following the motion of individual particles. Figure 6 displays the deposit patterns for droplets dried out at elevated temperatures. The droplet solution is the suspension of  $1.0 \mu\text{m}$  large silica particles at a concentration of 0.25%. From Figure 6 we see that on the substrate at room temperature, the temperature gradient is only originated from the evaporation of the droplet. This gradient is very small, so the Marangoni flow invokes only a negligible effect.<sup>1</sup> The replenish flow is dominated in the evaporating droplet, and particles are carried by this convection flow to form a ring which has accumulated the most particles. The deposit pattern on a heated substrate is, however, significantly different from the normal ring pattern. Though a ring is still formed at the contact line, more residual particles are left inside the dried spot. As the temperature of the substrate goes higher, the ring becomes thinner as less particles are incorporated into the ring. In contrast to the normal ring pattern obtained at room temperature where incorporated more than 90 percent of the particles, at 130°C this percentage is reduced to be less than 50%—the residual particles even form multilayered coating on the substrate. Noticeably, there is a region next to the ring, which may show depletion of particles (to be discussed below). Besides, the periphery of the droplet's base becomes irregular, being obviously a result of the non-uniform temperature field on the substrate.

For a droplet of water suspension on heated substrate, the droplet's surface is at a relatively lower temperature. Thus the surface tension becomes gradually larger toward the top of the droplet. This force arising from the surface tension gradient pulls water upward along the droplet surface.<sup>28</sup> As illustrated in Figure 7(a), this flow will drive particles that are located at the contact line to move up, implying the presence of a desorption process from the ring. More particles intend to stay in the liquid until the droplet finally dries out, leaving behind a quite homogenous coating inside the spot. Figure 7(b) shows sequential images of a solution droplet drying on a glass substrate held at 50°C. A remarkable feature is the presence of a region, directly to the ring, which shows depletion of particles. In Fig. 7(b) the depletion zone measures roughly  $30 \mu\text{m}$  wide. It occurs inevitably when the contact angle becomes sufficiently small, and the shrinking surface of the droplet experiences a 'jump'. From the video we see that at a moment when a portion of the liquid is evaporated and some particles have been driven to the edge, the contact line of liquid trepasses the deposited particles and



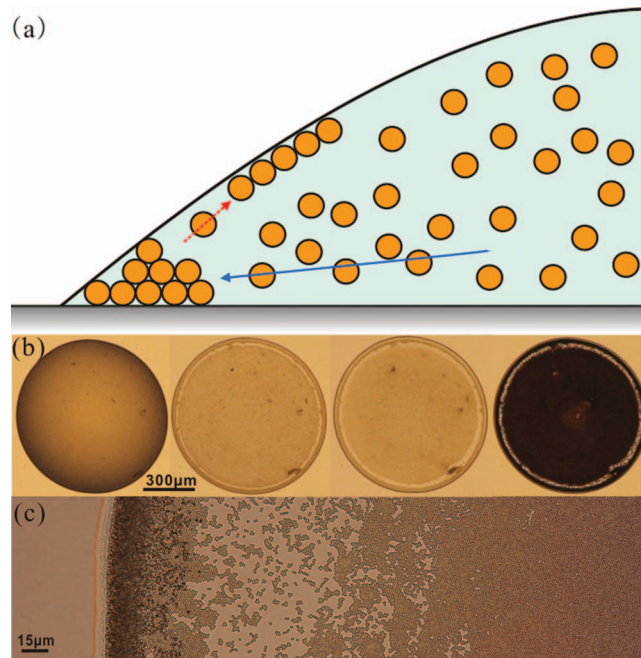


FIG. 7. (a) Schematic of Marangoni flow in a drying droplet containing particles on a heated substrate. The dashed arrow stands for Marangoni flow, and the solid arrow stands for the replenishing flow. (b) Sequential images in a time interval of 10 s for a droplet drying on glass at 50°C. (c) Local magnification of the deposit showing distinctly the ring, the depleted zone and the nearly close-packed monolayer in the central region. Colloidal mass concentration: 0.25 %; initial volume: 0.5  $\mu\text{L}$ .

extracts inward fiercely until it is pinned down at a new position. The region swept by the receding contact line is free of particles.

The presence of a depleted zone indicates that it will be a difficult challenge to applying the Marangoni flow to resolve the ring formation and at the same time to achieve a homogeneous particle deposition profile. However, we noticed that the Marangoni flow induces a floating layer of particles on liquid surface, which does produce a monolayered, and close-packed, deposition in the internal region of the stain (Figure 7(c)). Following the occurrence of the depleted zone due to slip motion of the contact line, the thinned liquid droplet has a limited height, and the particles floating on the liquid surface, when the temperature is properly chosen, are sufficiently mobile to self-assemble, leaving behind a close-packing monolayer in the central region.

The result in Figure 7 demonstrates that the Marangoni flow induced by surface tension gradient can be used to modify the particle deposition. It may hold promise for obtaining a homogeneous coating free of ring formation. As can be conceived, the temperature distribution inside an evaporating droplet on heated substrate can be prohibitively complicated, as the temperature gradient depends on many factors such as heat conductivity, droplet size and composition, etc. More meticulous research should be devoted to this problem when the Marangoni flow is to be applied for obtaining homogenous particle coatings instead of a coffee ring.

#### IV. CONCLUSION

In summary, we have investigated the ring formation process from a millimeter-sized drying sessile colloidal droplet on solid substrate with the aid of video microscopy. At the initial stage, particles are dragged by water flow to the pinned contact line to form a 2D nucleus in a line by line way, and this annular nucleus will be driven inward, though only slightly, by the shrinking surface. The number of particles added to the ring structure increases with time following the power law  $N \propto t^{3/(1+\lambda)}$ , where  $\lambda$  is a parameter related to the contact angle via  $\lambda = \frac{\pi - 2\theta_c}{2\pi - 2\theta_c}$ . For smaller contact

angle, the experimental value of  $\lambda$  agrees well with that obtained from model calculation, whereas for larger contact angle the experimental value of  $\lambda$  is obviously smaller.

At the later stage of evaporation the replenish flow is sufficiently fast that particles may come to the growth front in clusters, particles begin to pile on precedent layers, thus the deposit is amorphous. Meanwhile, at the edge the surface tension of the liquid exerts directly on the particles, thus the deposit is displaced inward and the outermost ordered part turns to be distorted. At the end of evaporation, the liquid membrane covering the deposited particles breaks up quite violently, which can also destroy the previously obtained ordered structure.

The Marangoni flow in droplets on heated substrate introduces a desorption path for particles along the liquid surface, which can partially resolve the ring. In the final stage of evaporation, residual particles floating on the liquid surface may leave behind a homogeneous monolayer coating inside the dried spot, however, a “jump” in the shrinking droplet surface area results in a depletion zone of particles. These results may be helpful for the development of strategies for suppressing the coffee ring effect and for obtaining homogeneous coatings from drying colloidal suspensions.

## ACKNOWLEDGMENTS

This work was financially supported by the Innovation Program of the Chinese Academy of Sciences, by the National Natural Science Foundation of China Grant nos. 11290161, 51172272 and 10904165, and by the National Basic Research Program of China grant nos. 2009CB930801 and 2012CB933002.

- <sup>1</sup> R. D. Deegan, O. Bakajin, T. F. Dupont, G. Huber, S. R. Nagel, and T. A. Witten, *Nature* **389**, 827 (1997).
- <sup>2</sup> R. D. Deegan, O. Bakajin, T. F. Dupont, G. Huber, S. R. Nagel, and T. A. Witten, *Phys. Rev. E* **62**, 756 (2000).
- <sup>3</sup> T. P. Bigioni, X. M. Lin, T. T. Nguyen, E. I. Corwin, T. A. Witten, and H. M. Jaeger, *Nat. Mater.* **5**, 265 (2006).
- <sup>4</sup> S. Choi, S. Stassi, A. P. Pisano, and T. I. Zohdi, *Langmuir* **26**, 11690 (2010).
- <sup>5</sup> T. Kajiyama, W. Kobayashi, T. Okuzono, and M. Doi, *J. Phys. Chem. B* **113**, 15460 (2009).
- <sup>6</sup> D. Kaya, V. A. Belyi, and M. Muthukumar, *J. Chem. Phys.* **133**, 114905 (2010).
- <sup>7</sup> Smalyukh, II, O. V. Zribi, J. C. Butler, O. D. Lavrentovich, and G. C. L. Wong, *Phys. Rev. Lett.* **96**, 177801 (2006).
- <sup>8</sup> D. Soltman and V. Subramanian, *Langmuir* **24**, 2224 (2008).
- <sup>9</sup> L. Zhang, H. Liu, Y. Zhao, X. Sun, Y. Wen, Y. Guo, X. Gao, C.-a. Di, G. Yu, and Y. Liu, *Adv. Mater.* **24**, 436 (2011).
- <sup>10</sup> B. J. de Gans and U. S. Schubert, *Langmuir* **20**, 7789 (2004).
- <sup>11</sup> V. Dugas, J. Broutin, and E. Souteyrand, *Langmuir* **21**, 9130 (2005).
- <sup>12</sup> B. J. de Gans, P. C. Duineveld, and U. S. Schubert, *Adv. Mater.* **16**, 203 (2004).
- <sup>13</sup> M. Naqshbandi, J. Canning, B. C. Gibson, M. M. Nash, and M. J. Crossley, *Nat. Commun.* **3**, 1188 (2012).
- <sup>14</sup> K. Sefiane, *J. Bionic Eng.* **7**, S82–S93 (2010).
- <sup>15</sup> W. D. Ristenpart, P. G. Kim, C. Domingues, J. Wan, and H. A. Stone, *Phys. Rev. Lett.* **99**, 234502 (2007).
- <sup>16</sup> S. Andrew, *J. Phys.: Condens. Matter* **23**, 083001 (2011).
- <sup>17</sup> F. Fan and K. J. Stebe, *Langmuir* **20**, 3062 (2004).
- <sup>18</sup> R. Dou and B. Derby, *Langmuir* **28**, 5331 (2012).
- <sup>19</sup> H. Hu and R. G. Larson, *J. Phys. Chem. B* **110**, 7090 (2006).
- <sup>20</sup> V. Truskett and K. J. Stebe, *Langmuir* **19**, 8271 (2003).
- <sup>21</sup> S. Maheshwari, L. Zhang, Y. Zhu, and H.-C. Chang, *Phys. Rev. Lett.* **100**, 044503 (2008).
- <sup>22</sup> T. Still, P. J. Yunker, and A. G. Yodh, *Langmuir* **28**, 4984 (2012).
- <sup>23</sup> C. S. Hodges, Y. Ding, and S. Biggs, *J. Colloid Interface Sci.* **352**, 99 (2010).
- <sup>24</sup> P. J. Yunker, T. Still, M. A. Lohr, and A. G. Yodh, *Nature* **476**, 308 (2011).
- <sup>25</sup> P. J. Yunker, M. A. Lohr, T. Still, A. Borodin, D. J. Durian, and A. G. Yodh, *Phys. Rev. Lett.* **110**, 035501 (2013).
- <sup>26</sup> A.-M. Cazabat and G. Guena, *Soft Matter* **6**, 2591 (2010).
- <sup>27</sup> Á. Marín, H. Gelderblom, D. Lohse, and J. Snoeijer, *Phys. Rev. Lett.* **107**, 085502 (2011).
- <sup>28</sup> H. Hu and R. G. Larson, *Langmuir* **21**, 3963 (2005).